Toll-like Receptor 2 Knockout Mice Showed Increased Periapical Lesion Size and Osteoclast Number

Raquel Assed Bezerra da Silva, DDS, MSc, PhD, Paula Dariana Fernandes Ferreira, DDS, MSc, Andiara De Rossi, DDS, MSc, PhD, Paulo Nelson-Filho, DDS, MSc, PhD, and Lea Assed Bezerra Silva, DDS, MSc, PhD

Abstract

Introduction: The aim of this study was to characterize the formation and progression of experimentally induced periapical lesions in TLR2 knockout (TLR2 KO) mice. **Methods:** Periapical lesions were induced in molars of 28 wild type (WT) and 27 TLR2 KO mice. After 7, 21, and 42 days, the animals were euthanized, and the mandibles were subjected to histotechnical processing. Hematoxylin-eosin–stained sections were examined under conventional light microscopy for the description of pulpal, apical, and periapical features and under fluorescence microscopy for the determination of the periapical lesion size. The subsequent sections were evaluated by tartrate resistant acid phosphatase histoenzymology (osteoclasts), Brown and Brenn staining (bacteria), and immunohistochemistry (RANK, RANKL, and OPG). Data were analyzed by the Mann-Whitney *U* and Kruskal-Wallis tests ($\alpha = 0.05$). **Results:** The WT group showed significant differences ($P < .05$) in the periapical lesion size and the osteoclast number between 7 and 42 days and between 21 and 42 days. In the TLR2 KO group, significant differences ($P < .05$) in the periapical lesion size and the osteoclast number were found between 7 days and the other periods. There was a significant difference ($P < .05$) between the 2 types of animal regarding the periapical lesion size, which was larger in the TLR2 KO animals. No significant differences ($P > .05$) were found between WT and TLR2 KO mice related to the pulpal, apical, and periapical features; bacteria localization; and immunohistochemical results (except for RANK expression). **Conclusions:** TLR2 KO animals developed larger periapical lesions with a greater number of osteoclasts, indicating the important role of this receptor in the host's immune and inflammatory response to root canal and periradicular infection. *(J Endod 2012;38:803–813)*

Key Words

knockout mice, osteoclastogenesis, periapical lesion, toll-like receptor 2

The activation of the host's response to inflammatory/infectious processes, such as apical periodontitis, is mediated by pattern-recognition receptors, such as nucleotide-binding oligomerization domain–like receptors and toll-like receptors (TLRs) (1, 2), which are expressed in different cell compartments that identify pathogen-associated molecular patterns. TLRs are type I transmembrane receptors that are strongly expressed in multiple cell types associated with infections of endodontic origin, such as neutrophils (3, 4), monocytes/macrophages, granulocytes, pulp fibroblasts, osteoclast precursors, and mesenchymal cells (1, 5), exerting an important role in the recognition of specific pathogen-derived components (6) and transmitting appropriate signals to the cells of the immune system (7). Also, these receptors are presented in the central nervous system, overexpressed in response to systemic or local insults (8), and in odontoblasts, participating in the inflammatory and immune response of the pulp tissue to pathogens (9).

The recognition of microorganisms, their components, and byproducts by TLRs stimulate the production of proinflammatory cytokines and costimulatory molecules, which are responsible for the different responses elicited by the identification of pathogen-associated molecular patterns (6). Several proinflammatory cytokines, such as interleukin (IL) 1, tumor necrosis factor α, and IL-6, are associated with the increase in the production of the receptor activator of nuclear factor kappa-B ligand (RANKL), a protein that regulates osteoclast formation, osteoclastgenesis, and bone resorption (1, 5).

TLR2 recognizes a variety of microbial components, namely lipoproteins/lipopeptides from different pathogens, and peptidoglycans and lipoteichoic acid from gram-positive bacteria and interacts with TLR1 and TLR6, which are involved in the discrimination of a subtle difference between triacyl and diacyl lipopeptides, respectively (6, 10, 11). TLR2 also participates in signal transduction activated by the bacterial LPS of some pathogens such as *Porphyromonas gingivalis* (12) and *Porphyromonas endodontalis* (13) through binding with the MD-2 auxiliary molecule (14). This receptor is largely expressed in blood leukocytes and different inflammatory cells, participating in the immune response to stimuli by increasing nuclear factor kappa B expression (15, 16). It has been shown that TLR2 is expressed by neutrophils (3, 4), mast cells (17), monocytes and macrophages (4, 18), T cells

From the Department of Pediatric Clinics, Preventive and Community Dentistry, School of Dentistry of Ribeirão Preto, University of São Paulo, Ribeirão Preto, São Paulo, Brazil.

This study is part of the master's dissertation of the second author (P.D.F.F.), who received a scholarship from the Brazilian Ministry of Health's Federal Agency for Support and Evaluation of Graduate Education (CAPES).

Address requests for reprints to Dr Raquel Assed Bezerra da Silva, Departamento de Clínica Infantil, Odontologia, Preventiva and Social, Faculdade de Odontologia de Ribeirão Preto, Universidade de São Paulo, Av. do Café, s/n Monte Alegre, 14040-904 Ribeirão Preto, SP, Brazil. E-mail address: raquel@forp.usp.br

0099-2399/$ - see front matter

doi:10.1016/j.joen.2012.03.017

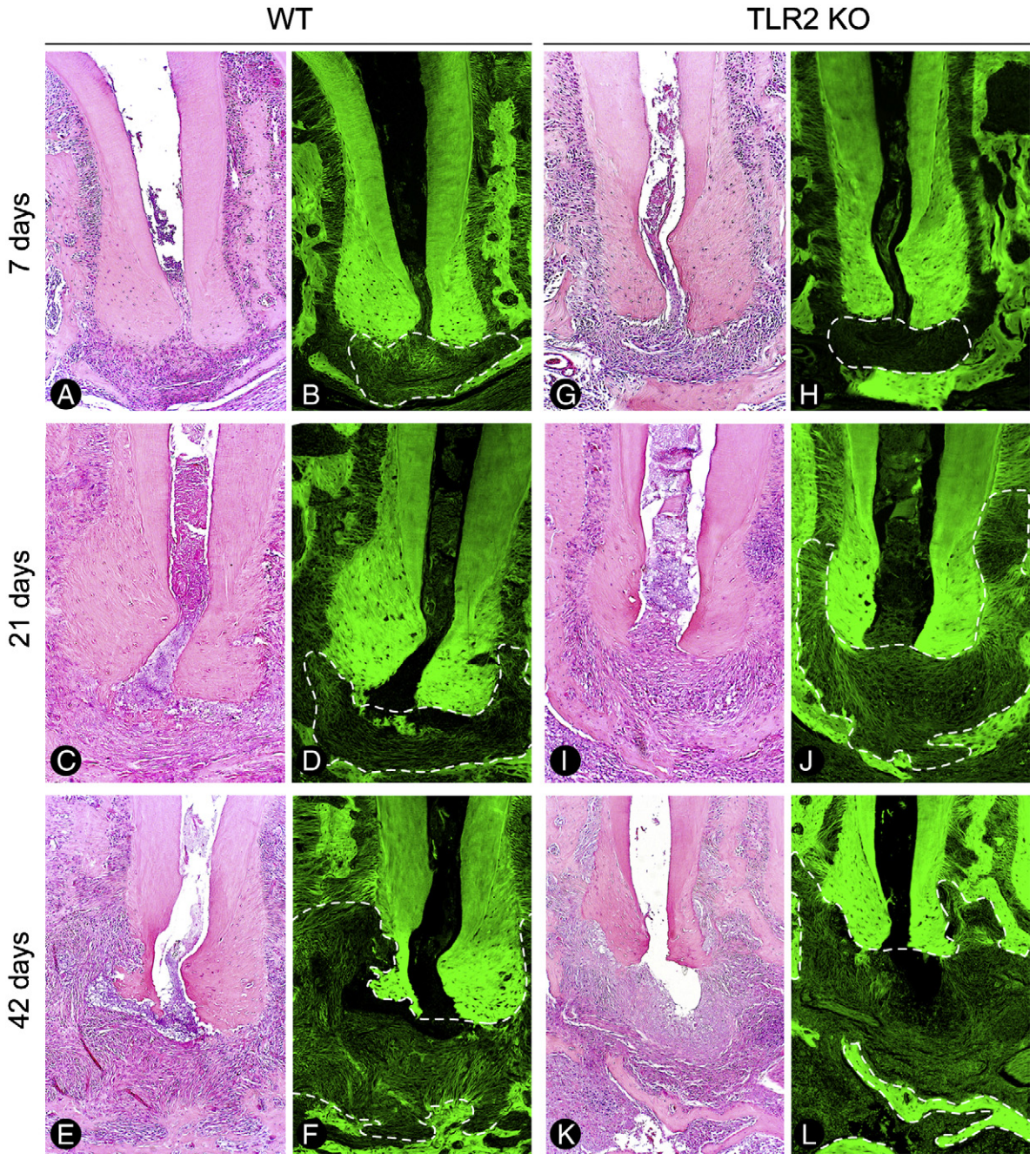

Figure 1. Representative HE-stained photomicrographs obtained 7, 21, and 42 days after the experimental induction of periapical lesions in WT and TLR2 KO animals for (*A*, *C*, *E*, *G*, *I*, and *K*) the description of pulpal, apical, and periapical features under conventional light microscopy and (*B*, *D*, *F*, *H*, *J*, and *L*) the determination of periapical lesion size under fluorescence microscopy (10× magnification).

(19), regulatory T cells (20), and B cells (21). Additionally, studies in murine pulp cells showed TLR2 expression in fibroblasts, odontoblasts, and dendritic cells (22, 23).

Chokechanachaisakul et al (24) found up-regulated TLR2 and TLR4 messenger RNA expression, suggesting the involvement of the innate immune mechanisms in the early pathogenesis of inflammatory processes in experimentally induced furcation lesions of endodontic origin in rat molars. Desai et al (25) reported TLR2 expression in different inflammatory cells of cysts and granulomas.

Although the role of TLR2 in pathogen recognition and activation of innate immunity has been shown, its function/participation in periapical lesion formation and progression has not yet been investigated. Therefore, the aim of this study was to characterize the formation and progression of experimentally induced periapical lesions in TLR2 knockout (TLR2 KO) mice compared with wild-type (WT) mice using conventional light microscopy, fluorescence microscopy, tartrate resistant acid phosphatase (TRAP) histoenzymology, Brown and Brenn staining, and immunohistochemistry. The hypothesis was that the TLR2 KO mice would develop smaller periapical lesions than the wild-type (WT) mice because of their deficiency in microbial recognition.

Materials and Methods

All animal procedures conformed to the applicable ethical guidelines and regulations of the University's Animal Research Ethics

TABLE 1. Periapical Lesion Size: Data and Comparison between Different Time Points in Both WT and TLR2 KO Animals and between Groups of Animals in the Same Periods of Time

	7 days M (Q1–Q3)	21 days M (Q1–Q3)	42 days M (Q1–Q3)	*P* value*
WT	55.860 (48,152.2–67,592.3)	71.450 (67,712.3–11,2791.9)	282.531 (219,768.5–301,503.6)	0,0002
TLR2 KO	86.810 (65,411.2–113,218.9)	262.538 (140,223–697,101)	687.342 (553755–727485)	<.0001
P†	.0101	.0027	.0002	

M, median; Q1, quartile 1; Q3: quartile 3.

*Mann-Whitney *U* test.

†Kruskal-Wallis test.

Committee (Process number 11.1.91.53.0). Age (6- to 8-week-old)- and weight (20 g)-matched male WT C57BL/6 (n = 28 animals, 56 teeth) and TLR2 KO B6.129-TLR2^{tm1kir}/J (n = 27 animals, 54 teeth) mice were used. The WT mice were obtained from the Animal's Facility of the School of Dentistry of Ribeirão Preto, University of São Paulo, Brazil, and the TLR2 KO mice were obtained from the Animal's Facility of the Department of Genetics of the Medical School of Ribeirão, University of São Paulo, Brazil, which originally purchased them from The Jackson Laboratory, Bar Harbor, Maine.

Periapical Lesion Induction

The protocol for the induction of periapical lesions was based on De Rossi et al (26). Briefly, the mice were anesthetized by an intramuscular injection of 10% ketamine hydrochloride (150 mg/kg of body weight) and 2% xylazine hydrochloride (7.5 mg/kg of body weight) in the thigh and mounted on a jaw retraction board.

Access to the pulp chamber of the lower first molars was gained with stainless-steel #1/4 round burs (GDK Densell Dental Technology, Buenos Aires, Argentina) in a low-speed handpiece, and the canals were localized and explored with a sterile #08 K-file (Les Fils D'Auguste Maillefer SA, Ballaigues, Switzerland) and left exposed to the oral cavity for lesion induction. The animals were randomly euthanized in a CO_2 chamber at days 7 (n = 8 WT, n = 10 TLR2 KO), 21 (n = 10 WT, n = 8 TLR2 KO), and 42 (n = 10 WT, n = 9 TLR2 KO).

Histotechnical Processing

The mandibles were removed, dissected, and sectioned to obtain individual roots, which were fixed in 10% phosphate-buffered formalin for 24 hours at room temperature, washed in running water for 4 hours, and demineralized in 4.13% ethylenediaminetetraacetic acid (pH = 7.2) at room temperature, which was changed every week until completing 30 days. Once decalcified, the specimens were washed in running water for 2 hours, dehydrated in ascending dilutions of ethanol, cleared in xylol, and embedded in paraffin. Longitudinal 5-μm-thick semiserial sections were cut in a mesiodistal orientation throughout the periapical lesion size.

In each group, representative sections were stained with hematoxylin-eosin (HE) for a descriptive analysis of the pulp tissue and apical and periapical regions under conventional light microscopy and for the determination of the periapical lesion size under fluorescence microscopy. The subsequent sections were subjected to TRAP histoenzymology for the identification of osteoclasts, Brown and Brenn staining for the localization of bacteria, and immunohistochemistry for the identification of osteoclastogenesis markers (RANK, RANKL, and OPG).

All analyses were performed by a single experienced examiner blinded to the groups using only sections containing the distal root of the mandibular first molar and simultaneously showing the tooth crown; the coronal, middle, and apical canal thirds; the apical foramen; and the alveolar bone. The Axio Imager.M1 microscope (Carl Zeiss MicroImaging GmbH, Göttingen, Germany) coupled to an AxioCam MRc5 camera (Carl Zeiss MicroImaging GmbH) was used for all analyses.

Descriptive Analysis of Pulpal, Apical, and Periapical Features under Conventional Light Microscopy

For this analysis, the following structures and parameters were assessed on HE-stained sections of each animal group for each experimental period (27): pulp tissue: necrosis (total or partial) and root canal content (presence or absence of necrotic pulp rests); apical cementum: external surface (regular or irregular) and characteristics and content (empty or containing necrotic pulp rests) of the cemental lacunae; periodontal ligament (PDL) space (apical): extension (normal or widened), characteristics of the inflammatory cell infiltrate, the presence of edema, and the presence of collagen fibers; and alveolar bone: the absence/presence of areas of resorption, osteoblasts, and osteoclasts.

Quantitative Analysis of Neutrophils

The number of neutrophils was counted under conventional light microscopy as described by De Rossi et al (26). A counting frame was centered at a fixed distance from the apical foramina of distal roots throughout the selected section of each different specimen of the HE-stained sections. In these delimited areas, the number of polymorphonuclear leukocytes was counted based on their identifying characteristics (ie, darkly stained cells with multilobed, horseshoe-shaped nuclei). The results were expressed as the number of cells.

Morphometric Analysis of Periapical Lesion Size under Fluorescence Microscopy

This analysis was performed in the same HE-stained sections using the microscope at ×10 magnification operating in the fluorescence mode (28) using the Alexa Fluor 488 filter (Carl Zeiss, Jena, Germany) with G365 excitation, FT395 reflectors, and LP420 emission. In each specimen, the size of the periapical lesion was outlined and measured in μm^2 using Axio Vision Rel 4.8 software (Carl Zeiss, Jena, Germany). Delineation was performed excluding intact tooth and bone structures (PDL, cementum, and alveolar bone), which are easily distinguishable by the strong green fluorescence, and including the areas of resorption and inflammatory infiltrate, which are identified by the absence of fluorescence and darkened appearance (28).

TRAP Histoenzymology

The analysis of TRAP activity was performed because this protein is a histochemical marker of osteoclasts. The sections were deparaffinized (2 xylol baths of 5 minutes each), hydrated (2 baths of 5 minutes each in100% ethanol; 1 bath of 2 minutes in 95%, 70%, and 50% ethanol; and 2 minutes in distilled water), immersed in a 50% alcohol/acetone solution for 1 minute, and left dry at room

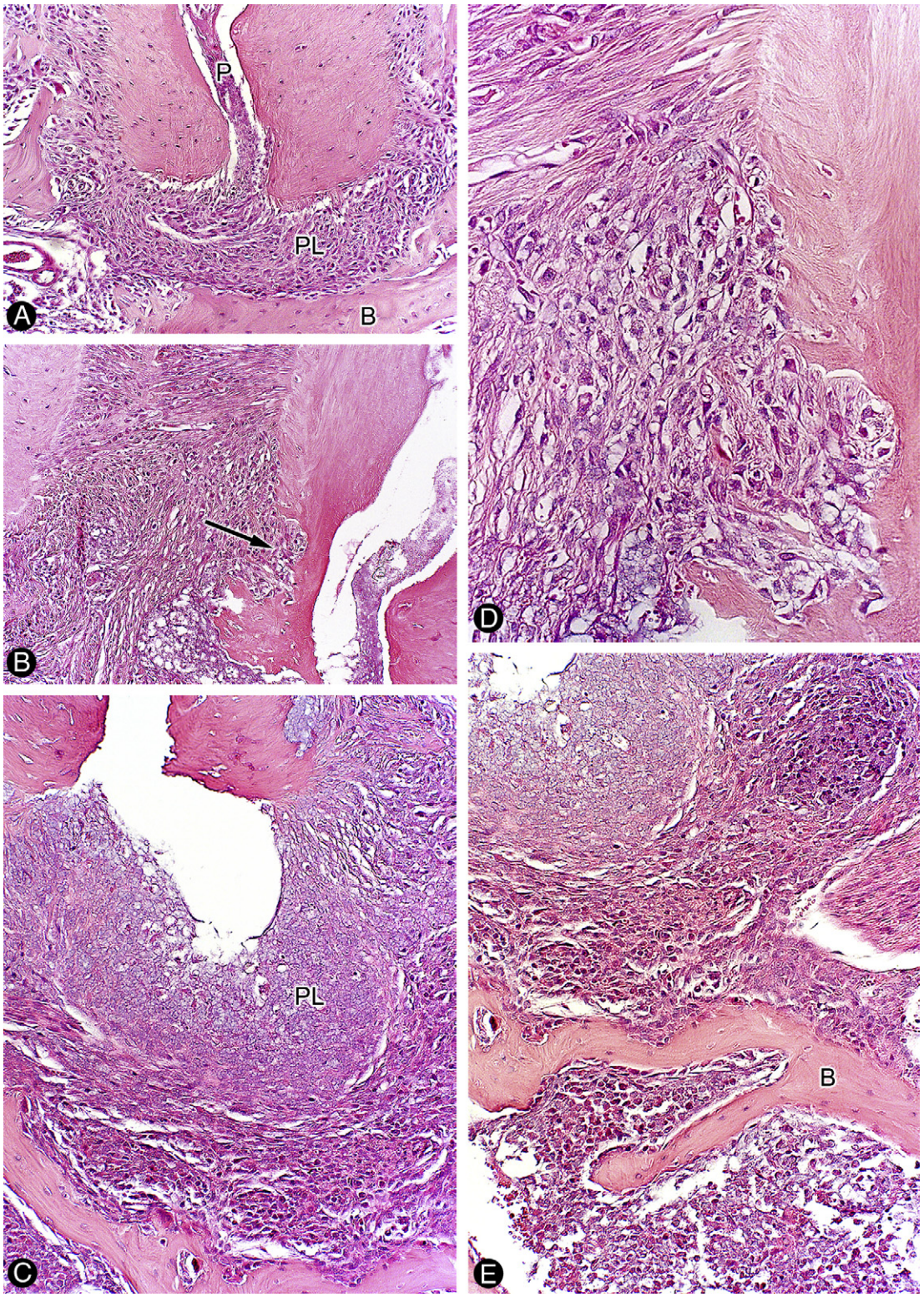

Figure 2. Representative HE-stained photomicrographs obtained 7, 21, and 42 days after the experimental induction of periapical lesions in WT and TLR2 KO animals for the descriptive analysis of the pulp tissue and apical and periapical regions under conventional light microscopy. (*A*) The apical and periapical region. P, necrotic pulp tissue; PL, slightly widened periodontal ligament; B, normal alveolar bone (HE Zeiss, 20×). (*B* and *D*) Root apex. Apical cementum with areas of resorption, fibrilar dissociation, and inflammatory cells (20× and 40× magnifications). (*C* and *E*) Apical and periapical region. Severely widened periodontal ligament (PL), intense fibrilar dissociation, accentuated edema, and extensive alveolar bone resorption (B) (20× magnification).

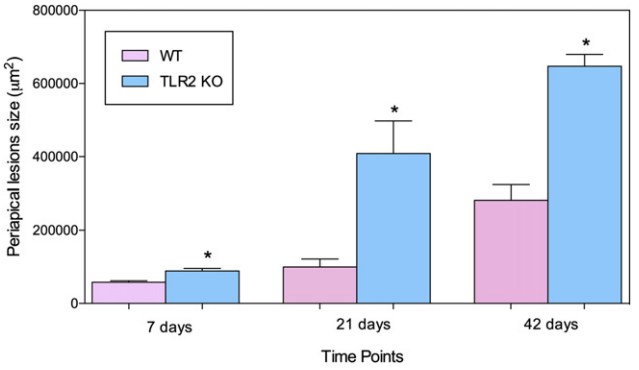

Figure 3. The measurement of the periapical lesion size in both groups (WT and TLR2 KO animals) at different time points (7, 21, and 42 days). *Significant statistical difference.

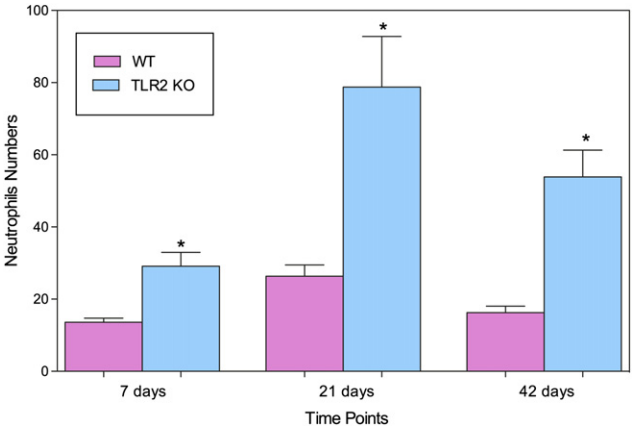

Figure 4. The measurement of the neutrophil number in both groups (WT and TLR2 KO animals) at different time points (7, 21, and 42 days). *Significant statistical difference.

temperature. Next, a solution prepared with 10 mL acetic acid buffer, 0.1 mL N-N-dimethylformamide, 5 mg Fast Red Violet LB Salt, and 1 mg Naphthol AS-BI phosphoric acid was pipetted onto the sections, which were maintained in a light-proof environment at 37°C for approximately 35 minutes. After incubation, the sections were counterstained with aniline blue for 1 minute, mounted on microscopic slides, and examined with the microscope under reflected light. The quantitative analysis of the number of osteoclasts was determined by counting the number of multinucleate TRAP-positive cells in the resorption lacunae in direct contact with the alveolar bone around the periapical lesion. The results were expressed as the number of cells per millimeter of resorbed bone length.

Brown and Brenn Staining

Brown and Brenn staining (29) was used to determine the presence or absence of bacteria and their location in the tooth crown, root canal system, and periapical tissues (ie, cementum, PDL space, and alveolar bone). The following 6-point scoring system modified from De Rossi et al (26) was used to assess the bacterial penetration from the tooth crown toward the periapical lesion: 0, no bacteria; 1, bacteria in the tooth crown; 2, bacteria in the coronal third; 3, bacteria in the middle third; 4, bacteria in the apical third; and 5, bacteria in the periapical lesion.

Immunohistochemical Analysis

The sections were deparaffinized and hydrated as described previously. Antigenic recovery was performed by immersing the slides in citrate buffer (pH = 6.0) and heating in a microwave oven at maximum power (2 cycles of 10 seconds each). After cooling to room temperature, the slides were washed twice (10 minutes each time) with phosphate-buffered saline (PBS) and rinsed for 10 minutes with 0.5% PBS/Triton solution (Sigma-Aldrich Corp, St Louis, MO). Endogenous peroxidase was then blocked by immersing the slides in a 3% hydrogen peroxide solution for 20 minutes under the protection of light, followed by rinsing in PBS and PBS/Triton solution as described earlier. Unspecific ligations were blocked by immersing the slides in a 1% bovine serum albumin/PBS solution for 30 minutes. Then, the slides were incubated overnight at 4°C with the primary antibodies diluted in 1% bovine serum albumin: anti-RANK (polyclonal rabbit antibody; Santa Cruz Biotechnology Inc, Santa Cruz, CA; 1:700 dilution) or anti-RANKL (polyclonal goat antibody, Santa Cruz Biotechnology Inc, 1:400 dilution) or anti-OPG (polyclonal goat antibody, Santa Cruz Biotechnology Inc, 1:700 dilution). After returning to room temperature, the slides were washed as described previously and incubated with biotinylated secondary antibody (goat antirabbit immunoglobulin G-B and rabbit antigoat immunoglobulin G-B, Santa Cruz Biotechnology Inc, 1:200 dilution) for 1 hour at room temperature. After new washing with PBS and PBS/Triton solution, the streptavidin-biotin-peroxidase complex (ABC Kit, Vecstain; Vector Laboratories Inc, Burlingame, CA) was added for 30 minutes. The slides were washed again with PBS and PBS/Triton solution, and the reaction was visualized on a chromogen 3,3' diaminobenzidine tetrahydrochloride hydrate (DAB; Sigma-Aldrich Corp, St Louis, MO) added with 3% hydrogen peroxide in PBS for 1 minute. The slides were counterstained with Harris hematoxylin for 10 seconds, washed in running water, washed in ammoniacal water for 30 seconds, washed again in running water, cleared, dehydrated, and covered with coverslips. The identification of the markers for osteoclastogenesis was performed under reflected light. Results were expressed in a qualitative manner, considering the presence/absence and localization of immunostaining.

TABLE 2. The Number of Neutrophils: Data and Comparison between Different Time Points in Both WT and TLR2 KO Animals and between Groups of Animals in the Same Periods of Time

	Wild		TLR2		
	Median	Q1–Q3	Median	Q1–Q3	*P* value*
7 days	13.0	11.5–15.7	25.5	22.0–40.5	.0269
21 days	25.0	21.0–33.0	69.0	56.0–81.0	.0246
42 days	14.0	13.0–18.0	50.0	40.0–70.0	.0075
P value†	.0069		.0033		

*Mann-Whitney *U* test comparing both WT and TLR2 mice.

†Kruskal-Wallis test comparing the time within each group of animals.

Statistical Analysis

The results for periapical lesion size, the number of osteoclasts, and neutrophils were analyzed using SAS software (Statistical Analysis System) for Windows version 9.1.3 (SAS Institute Inc, Cary, NC). Comparisons among the experimental periods (7, 21, and 42 days) within the same animal group (WT or TLR2 KO) were performed by the Mann-Whitney *U* test and the Dunn post-test. A comparison between the groups for each experimental period was performed by the Kruskal-Wallis test. A significance level of 5% was set for all analyses.

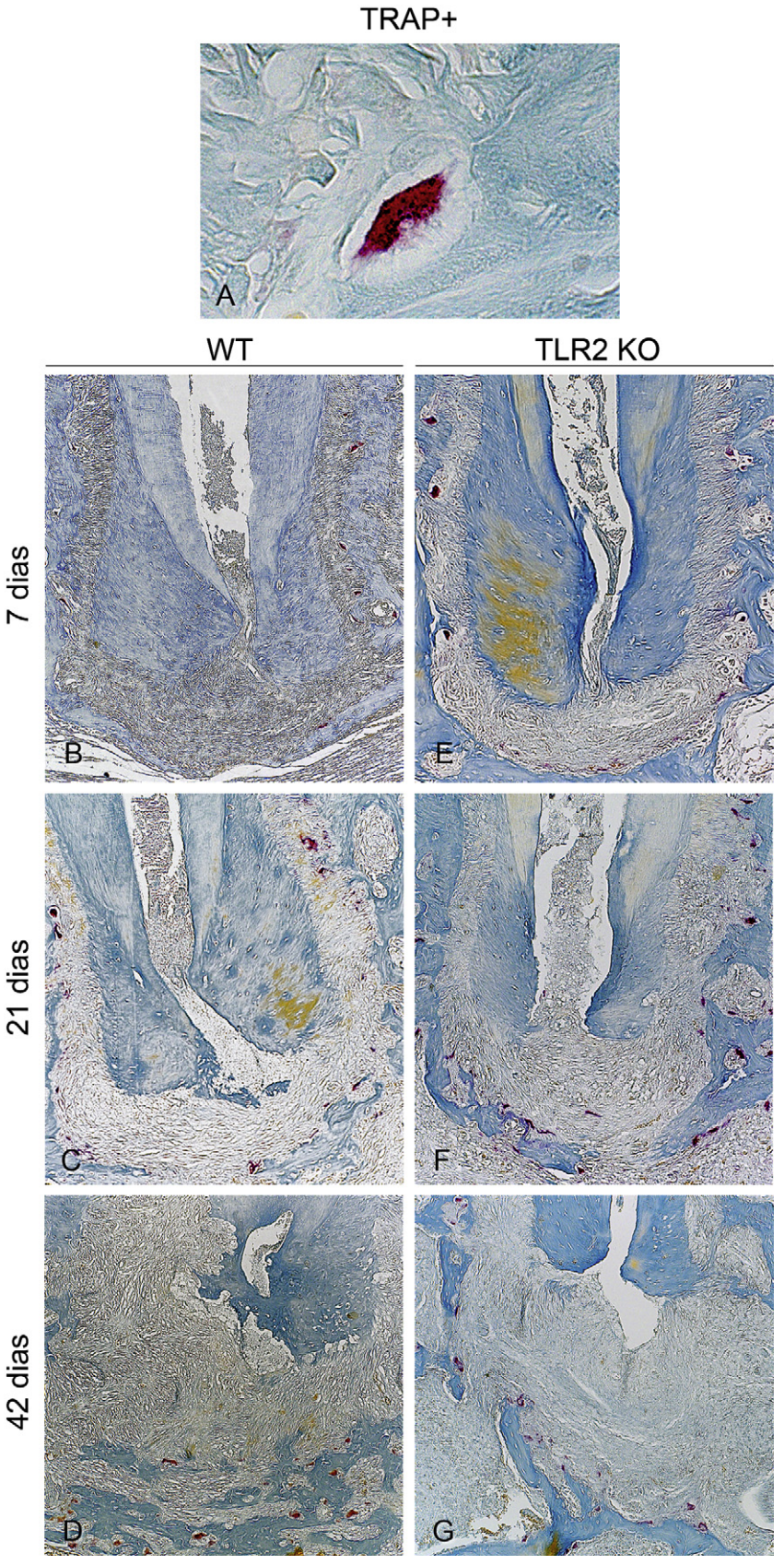

Figure 5. Representative photomicrographs obtained 7, 21, and 42 days after experimental induction of periapical lesions in (*B*, *C*, and *D*) WT and (*E–G*) TLR2 KO animals and stained for TRAP histoenzymology for the identification and counting of the number of osteoclasts. An osteoclastic cell can be seen in *A* (10× and 100× magnifications).

Results

Descriptive Analysis of Pulpal, Apical, and Periapical Features and Morphometric Analysis of Periapical Lesion Size

In the WT animals, necrosis of the entire pulp tissue was observed 7 days after the coronal opening and root canal contamination. The cemental surface was regular, the PDL space was slightly widened with occasional inflammatory cells, and the alveolar bone was normal. The median of the periapical lesion size in this period was 55.860 μm^2 (Fig. 1*A* and *B*). At 21 days, necrosis of the entire pulp tissue and a variable amount of necrotic pulp rests were found in the root canals. The apical cementum surface was irregular and presented resorption lacunae either empty or with necrotic pulp rests. The PDL space was severely widened, with generalized edema and inflammatory cells scattered throughout the examined region. The alveolar bone exhibited areas of resorption with no osteoblasts on its surface. The median of the periapical lesion size in this period was 71.450 μm^2 (Fig. 1*C* and *D*). At 42 days, the major histological features were pulp necrosis in the 3 root canal thirds; a severely widened PDL space with a dense, predominantly mononuclear inflammatory infiltrate; and denuded alveolar bone. The median of the periapical lesion size in this period was 282.531 μm^2 (Fig. 1*E* and *F*). There were statistically significant differences between 7 and 42 days and between 21 and 42 days ($P < .05$).

In the TLR2 KO animals, necrosis of the entire pulp tissue was also observed 7 days after the coronal opening and root canal contamination. The cemental surface was regular, the PDL space was severely widened with occasional inflammatory cells, and the alveolar bone was normal. The median of the periapical lesion size in this period was 86.810 μm^2 (Fig. 1*G* and *H*). At 21 days, pulp necrosis was observed in all root canal thirds. The apical cementum surface was irregular, and the PDL space was severely widened, exhibiting a mixed inflammatory infiltrate, generalized edema, and intense fibrillar dissociation. The median of the periapical lesion size in this period was 262.538 μm^2 (Fig. 1*I* and *J*). At 42 days, the pulp tissue was completely necrotic. The apical cementum surface was irregular and exhibited large empty resorption lacunae. The PDL space was severely widened, exhibiting an inflammatory cell infiltrate. The alveolar bone presented areas of resorption. The median of the periapical lesion size in this period was 687.342 μm^2 (Fig. 1*L* and *M*). Statistically significant differences were found between 7 and 21 days and between 7 and 42 days ($P < .05$).

The analysis of data revealed a significant difference ($P < .05$) between the 2 types of animals with respect to the periapical lesion size, which was larger in the TLR2 KO animals. Data and comparison of periapical lesion size between different time points in both the WT and TLR2 KO animals and between groups of animals in the same periods of time are represented in Table 1 and Figure 3. The results show that, in both WT and TLR2 KO animals and all time points (7, 21, and 42 days after the experimental induction of periapical lesions), the apical and periapical region showed necrotic pulp tissue (P in Fig. 2*A*), slightly widened periodontal ligament, and normal alveolar bone (PL and B in Fig. 2*A*).

Within the same time points and groups of animals, the root apex showed apical cementum with areas of resorption (arrow in Fig. 2*B*), fibrillar dissociation, and inflammatory cells (Fig. 2*D*). The apical and periapical region also showed a severely widened periodontal ligament (PL in Fig. 2*C*), intense fibrillar dissociation, accentuated edema, and extensive alveolar bone resorption (B in Fig. 2*E*).

Quantitative Analysis of Neutrophils

Data related to the neutrophil number in the periapical lesions are shown in Table 2. Regarding WT animals, the cell number increased when comparing day 21 with day 7, with a statistically significant difference ($P < .05$). After that, at day 42, the number of neutrophils decreased again in a similar level when compared with the initial time point although without a significant difference between them ($P > .05$). The median numbers at days 7, 21, and 42 were 13, 25 and 14, respectively. In a similar way, the number of neutrophils on TLR2 mice increased from day 7 to 21, with a decrease on day 42. Statistically significant differences were found among all time points ($P < .05$). Comparing the 2 types of animals, there was a significant difference regarding all time points ($P < .05$) with a larger number of neutrophils in TLR2 mice. Figure 4 represents the comparison among times points (7, 21, and 42 days) and group of animals (WT and TLR2 KO) and the statistical analyses of the results.

TRAP Histoenzymology

Regarding the number of osteoclasts, statistically significant differences were observed between 7 and 42 days and between 21 and 42 days in the WT group ($P < .05$), whereas in the TLR2 KO group significant differences ($P < .05$) were found between 7 and 21 days and between 7 and 42 days. In addition, statistically significant differences were found among all periods within each group regardless of the type of animal (WT and TLR2 KO, $P < .05$, Fig. 5). Table 3 shows the median values (ie, Q1 and Q3 related to the number of osteoclasts in the periapical lesions). It also shows the statistical analyses among the different time points (7, 21, and 42 days) in both groups (WT and TLR2 KO animals). Comparison among time points (7, 21, and 42 days) and groups of animals (WT and TLR2 KO) and statistical analyses are represented in Figure 6.

Brown and Brenn Staining

All specimens of both groups, in all time points, were scored for the presence of bacteria in the root canal system and periapical region. High bacterial counts were found in the tooth crown and in the coronal root canal third, with microorganisms frequently penetrating the

TABLE 3. The Number of Osteoclasts: Data and Comparison between Different Time Points in Both WT and TLR2 KO Animals and between Groups of Animals in the Same Periods of Time

	7 days M (Q1–Q3)	21 days M (Q1–Q3)	42 days M (Q1–Q3)	*P* value*
WT	5.5 (5.5–10)	8.25 (5.5–12)	19.0 (14.0–33.0)	.0016
TLR2 KO	11.0 (8.5–13.5)	32.5 (18.5–41.5)	86.0 (53.5–100.5)	<.0001
P value†	.0469	.0002	.0008	

M, median; Q1, quartile 1; Q3, quartile 3.

*Mann-Whitney *U* test.

†Kruskal-Wallis test.

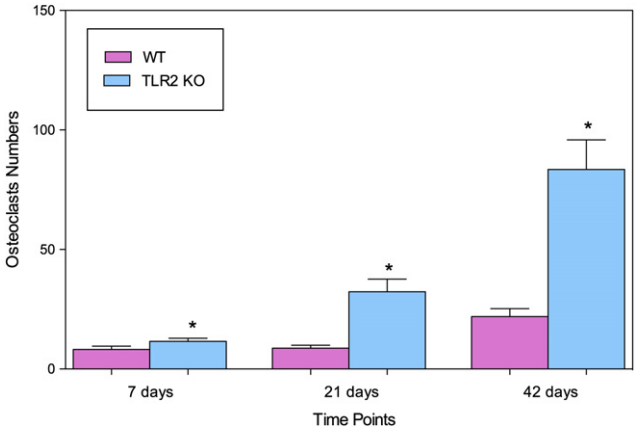

Figure 6. The measurement of the osteoclast numbers in both groups (WT and TLR2 KO animals) at different time points (7, 21, and 42 days). *Significant statistical difference.

dentinal tubules and the inter-radicular region. No specimen exhibited bacteria in the periapical lesion (Fig. 7).

Immunohistochemical Analysis

In the WT group, RANKL immunostaining was detected at 7 and 21 days, mainly in the apical foramen region and inside the periapical lesion. In only 1 specimen of this group, at 7 days, RANKL immunostaining was detected in the region corresponding to the periphery of the periapical lesion. In the TLR2 KO group, RANKL immunostaining was observed in the 3 experimental periods only in the apical foramen region and inside the periapical lesion. Positive immunoreactivity to RANK was observed only in the WT group, mainly at the apical foramen level and occasionally inside the periapical lesion.

Except for the 7-day experimental period in the TLR2 KO group, OPG immunostaining was detected in all other periods in both groups. OPG immunostaining was observed mainly inside the periapical lesion and at its periphery, but some specimens also exhibited positive immunoreactivity to OPG in the apical foramen region (Fig. 8).

Discussion

The hypothesis tested in this study was that the TLR2 KO mice would develop smaller periapical lesions than the WT mice because of their deficiency in microbial recognition. However, unlike the expected, the TLR2 KO animals presented surprisingly larger periapical lesions than the WT animals.

In the present study, although the presence/localization of microorganisms and the description of pulpal, apical, and periapical features were similar in both groups of animals, the analysis of the HE-stained sections by fluorescence microscopy revealed a progressive increase in periapical lesion size from the earliest (7 days) toward the latest (42 days) experimental period in both the WT and TLR2 KO groups, with medians of 71,450.4 μm^2 and 262,538 μm^2 in the intermediate period (21 days), respectively. It is important to mention that the medians of the periapical lesions in the TLR2 KO group were significantly larger ($P < .05$) than those in the WT group at all experimental periods.

Regarding the fact that TLR2 KO mice developed larger periapical lesions, it could be hypothesized that these mice presented an overexpression of other TLRs because of the absence of TLR2. Additionally, it is possible that other signaling pathways had been activated, for example, after binding of the auxiliary molecule MD-2 to TLR4 receptor because the amount of MD-2 in TLR2 KO mice is sufficient to maintain TLR4 functions (14). Moreover, a possible increase in the levels of proinflammatory cytokines, as observed by Zhu et al (30), would contribute to the progression of the periapical lesions and the increase of their size in the TLR2 KO animals. On the other hand, the results of the present study were the opposite of those shown by Hou et al (31), who described that TLR4-deficient mice, after pulp contamination, developed smaller periapical lesions and presented expression of several cytokines. Therefore, this supports that LPS is possibly a more relevant mediator of periapical lesion formation than other signals related to TLR2 activation.

Little is known about the effect of TLR2 receptors on the repair or progression of infections of different etiologies. Considering the limitations of the present study, it may be speculated that the silence of TLR2, which is strongly related to the recognition of gram-positive pathogens and their byproducts, led to a more intense activation of other TLRs. A greater stimulation of TLR4, for example, could enhance the deleterious effects of bacterial LPS, leading to a greater progression of the periapical lesions. Some studies, especially in periodontics, corroborate this hypothesis because increased severity of periodontitis after *Aggregatibacter actinomycetemcomitans* infection has been observed in TLR2 KO mice (32).

In addition, based on TLR2 expression in periapical lesions in humans and the existing knowledge of the regulatory mechanisms involving TLRs (33, 34), Desai et al (25) suggested that the inhibition of some routes of action of these receptors would cause overexpression of other TLRs by immune system cells present in the periapical lesions. According to Graves et al (35), the inhibition of the immune response in lesions of endodontic origin causes an increase in the susceptibility to bacterial infection. Those authors also stated that the use of specific inhibitors of inflammatory cytokines tends to cause the formation of larger osteolytic lesions because they compromise the ability of the host to protect itself from the reservoir of bacteria in the necrotic pulp, as observed in the present study in the TLR2 KO mice. In another study (36), the inhibition of chemokine (C-C motif) receptor 2 (CCR2) also caused an increase of the periapical lesion size in mice.

RANKL and OPG expression in periapical lesions has been shown in rodents and humans (37–40), suggesting that the RANK/RANKL/OPG system has an important role in the development and progression of periapical lesions. Although Menezes et al (39) found a predominance of RANKL expression in active periapical lesions, in the present study, strong immunostaining occurred in both groups of animals although this marker was not quantified by specific biochemical (enzyme-linked immunosorbent assay) and molecular (polymerase chain reaction) methods.

RANKL and OPG immunostaining was similar in both groups at the 3 experimental periods, and, surprisingly, no positive immunoreactivity to RANK was observed in the TLR2 KO group. Although the ideal approach would have been to quantify the expression level and confirm the absence of those markers using the polymerase chain reaction–enzyme-linked immunosorbent assay system, the results of the present study suggest that the increase of the periapical lesion size in the TLR2 KO animals may be related to another pathway of the activation of bone resorption independent of the RANK/RANKL/OPG system.

It is important to emphasize that the lack of studies evaluating the presence of osteoclasts and the expression of osteoclastogenesis markers in periapical lesions induced in TLR2 KO animals prevent the comparison of the present results with previous findings in the literature. Further research should elucidate the molecular mechanisms of compensation, stimulation, and inhibition of bone resorption, allowing the silencing of multiple genes that act on the recognition of microorganisms and the activation of the immune and inflammatory systems

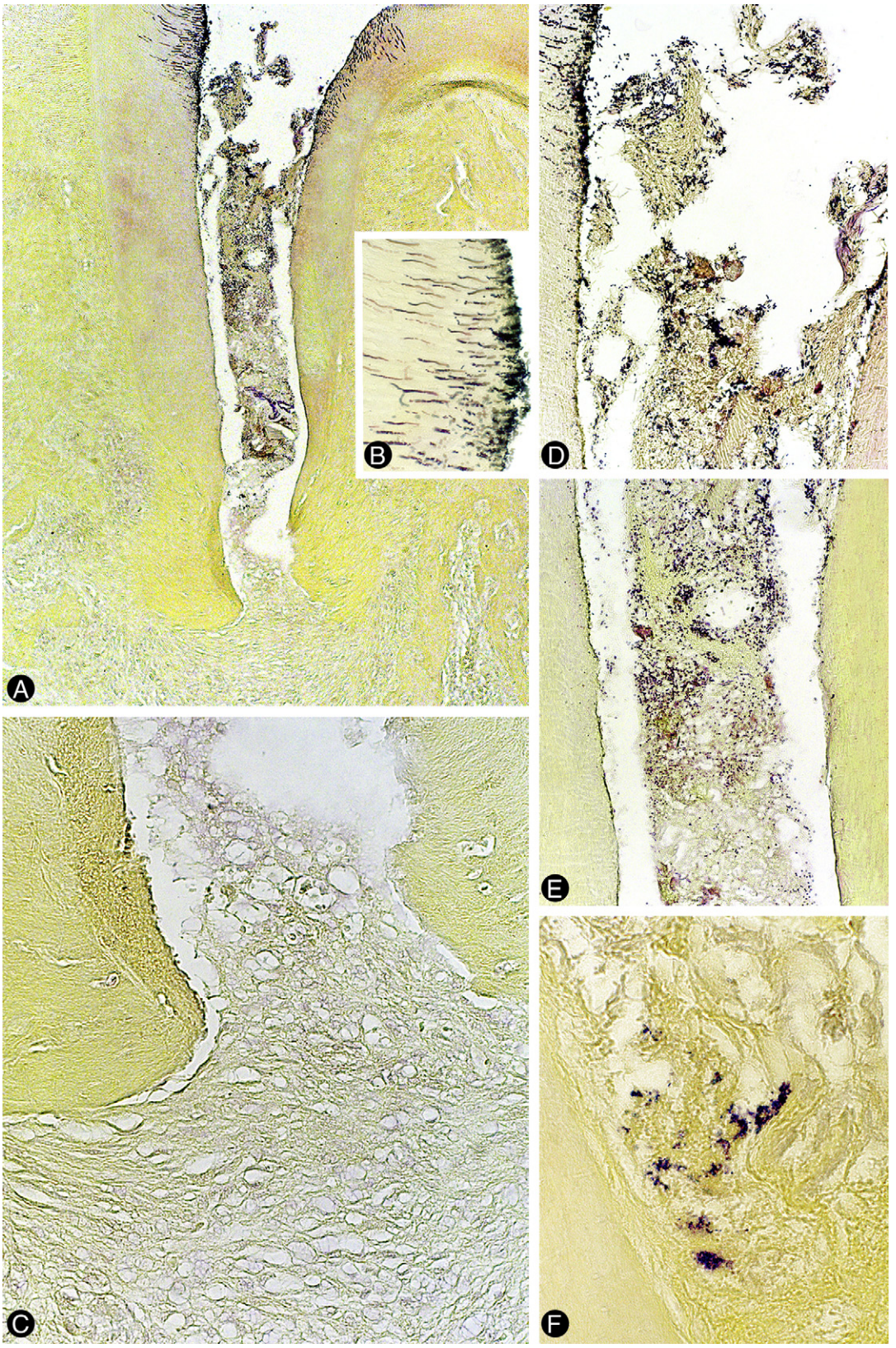

Figure 7. Representative photomicrographs of the different areas of the root canal system and apical and periapical region obtained 7, 21, and 42 days after the experimental induction of periapical lesions in WT and TLR2 KO and subjected to Brown and Brenn staining. (*A*) Different microbial morphotypes can be seen along the main root canal and the periradicular dentin (10×). (*B*) Detail of *A* showing the dentinal tubules with the intense presence of bacteria (100×). (*C*) Detail of *A* showing the absence of microorganisms in the periapical region (63×). (*D*) Coronal, (*E*) middle, and (*F*) apical root canal thirds with pulp tissue necrosis and heavy presence of gram-positive and gram-negative microorganisms (40× and 100× magnifications).

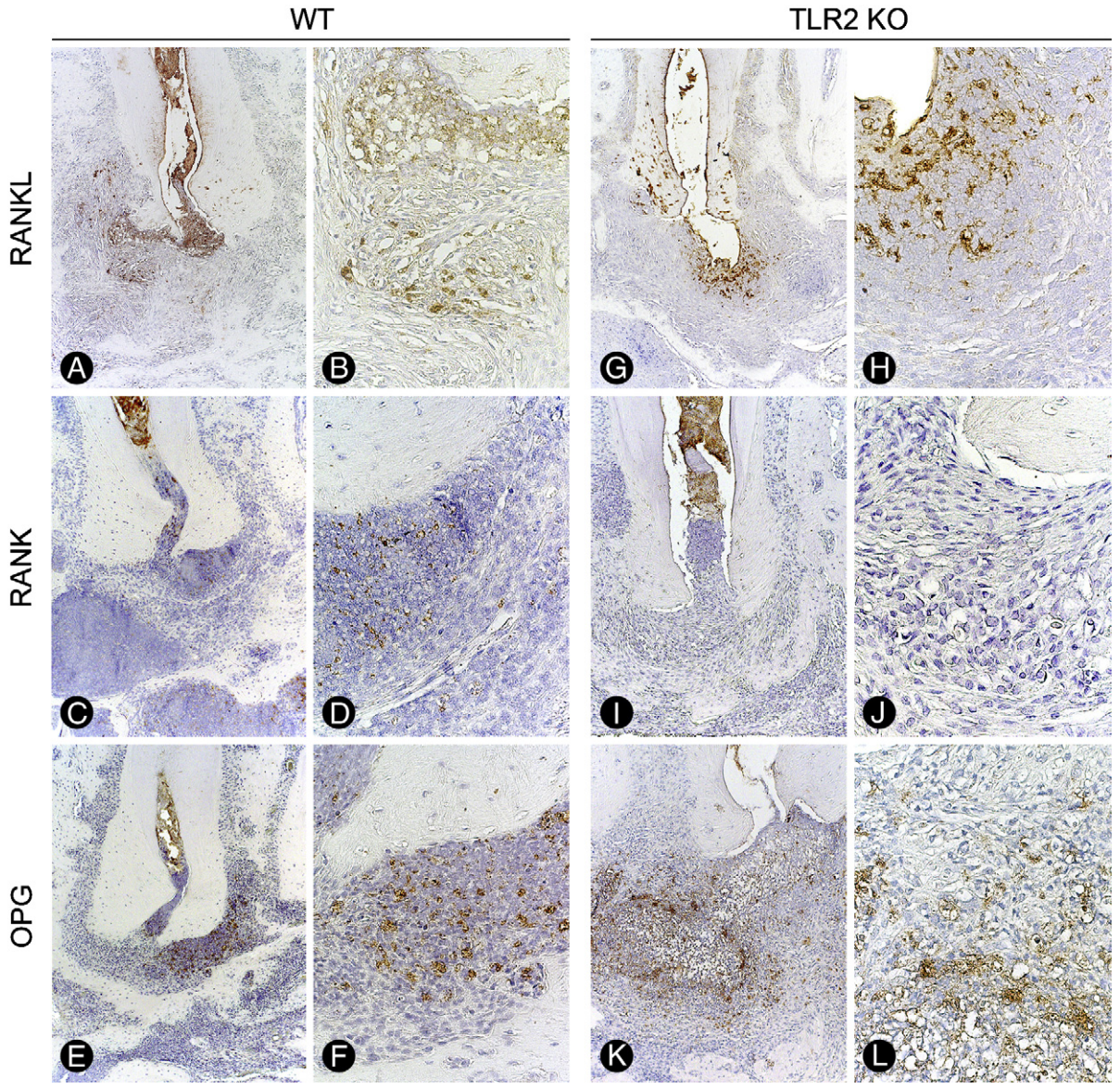

Figure 8. Representative photomicrographs obtained 7, 21, and 42 days after the experimental induction of periapical lesions in (*A–F*) WT and (*G–L*) TLR2 KO animals and stained for immunohistochemistry for the identification of osteoclastogenesis markers (RANK, RANKL, and OPG) (10× and 40× magnifications).

involved in the development and progression of periapical lesions, which remain unknown. Based on the findings of the present study, it may be concluded that TLR2 KO mice developed larger periapical lesions with a greater number of osteoclasts compared with the WT animals, indicating the important effect of this receptor during the immune and inflammatory response against the infection of root canal system and periapical tissues.

Acknowledgments

The authors deny any conflicts of interest related to this study.

References

1. Hirao K, Yumoto H, Takahashi K, Mukai K, Nakanishi T, Matsuo T. Roles of TLR2, TLR4, NOD2, and NOD1 in pulp fibroblasts. J Dent Res 2009;88:762–7.
2. Kawai T, Akira S. The roles of TLRs, RLRs and NLRs in pathogen recognition. Int Immunol 2009;21:317–37.
3. Hayashi F, Means TK, Luster AD. Toll-like receptors stimulate human neutrophil function. Blood 2003;102:2660–9.
4. Nilsen N, Nonstad U, Khan N, et al. Lipopolysaccharide and double-stranded RNA up-regulate toll-like receptor 2 independently of myeloid differentiation factor 88. J Biol Chem 2004;279:39727–35.
5. Bar-Shavit Z. Taking a toll on the bones: regulation of bone metabolism by innate immune regulators. Autoimmunity 2008;41:195–203.
6. Takeda K, Akira S. Toll-like receptors in innate immunity. Int Immunol 2005;17: 1–14.
7. Medzhitov R, Preston-Hurlburt P, Janeway CA Jr. A human homologue of the Drosophila Toll protein signals activation of adaptive immunity. Nature 1997;388: 394–7.
8. Medzhitov R. Toll-like receptors and innate immunity. Nat Rev Immunol 2001;1. 135–5.
9. Farges JC, Carrouel F, Keller JF, et al. Cytokine production by human odontoblast-like cells upon Toll-like receptor-2 engagement. Immunobiology 2011;216: 513–7.
10. Takeuchi O, Kawai T, Mühlradt PF, et al. Discrimination of bacterial lipoproteins by Toll-like receptor 6. Int Immunol 2001;13:933–40.
11. Takeuchi O, Sato S, Horiuchi T, et al. Cutting edge: role of Toll-like receptor 1 in mediating immune response to microbial lipoproteins. J Immunol 2002;169:10–4.

12. Yamagishi VT, Torneck CD, Friedman S, Huang GT, Glogauer M. Blockade of TLR2 inhibits Porphyromonas gingivalis suppression of mineralized matrix formation by human dental pulp stem cells. J Endod 2011;37:812–8.
13. Tang Y, Sun F, Li X, Zhou Y, Yin S, Zhou X. *Porphyromonas endodontalis* lipopolysaccharides induce RANKL by mouse osteoblast in a way different from that of Escherichia coli lipopolysaccharide. J Endod 2011;37:1653–8.
14. Dziarski R, Gupta D. Role of MD-2 in TLR2- and TLR4-mediated recognition of Gram-negative and Gram-positive bacteria and activation of chemokine genes. J Endotoxin Res 2000;6:401–5.
15. Akira S, Uematsu S, Takeuchi O. Pathogen recognition and innate immunity. Cell 2006;124:783–801.
16. Beutler BA. TLRs and innate immunity. Blood 2009;113:1399–407.
17. McCurdy JD, Olynych TJ, Maher LH, Marshall JS. Cutting edge: distinct Toll-like receptor 2 activators selectively induce different classes of mediator production from human mast cells. J Immunol 2003;170:1625–9.
18. Chokechanachaisakul U, Kaneko T, Yamanaka Y, et al. Gene expression analysis of resident macrophages in lipopolysaccharide-stimulated rat molar pulps. J Endod 2011;37:1258–63.
19. Komai-Koma M, Jones L, Ogg GS, Xu D, Liew FY. TLR2 is expressed on activated T cells as a costimulatory receptor. Proc Natl Acad Sci U S A 2004;101: 3029–34.
20. Liu H, Komai-Koma M, Xu D, Liew FY. Toll-like receptor 2 signaling modulates the functions of CD4+ CD25+ regulatory T cells. Proc Natl Acad Sci U S A 2006;103: 7048–53.
21. Vasilevsky S, Chattopadhyay G, Colino J, et al. B and CD4+ T-cell expression of TLR2 is critical for optimal induction of a T-cell-dependent humoral immune response to intact *Streptococcus pneumoniae*. Eur J Immunol 2008;38:3316–26.
22. Staquet MJ, Durand SH, Colomb E, et al. Different roles of odontoblasts and fibroblasts in immunity. J Dent Res 2008;87:256–61.
23. Keller JF, Carrouel F, Colomb E, et al. Toll-like receptor 2 activation by lipoteichoic acid induces differential production of pro-inflammatory cytokines in human odontoblasts, dental pulp fibroblasts and immature dendritic cells. Immunobiology 2010;215:53–9.
24. Chokechanachaisakul U, Kaneko T, Okiji T, et al. Increased gene expression of toll-like receptors and antigen-presenting cell-related molecules in the onset of experimentally induced furcation lesions of endodontic origin in rat molars. J Endod 2010;36:251–5.
25. Desai SV, Love RM, Rich AM, Seymour GJ. Toll-like receptor 2 expression in refractory periapical lesions. Int Endod J 2011;44:907–16.
26. De Rossi A, Rocha LB, Rossi MA. Interferon-gamma, interleukin-10, Intercellular adhesion molecule-1, and chemokine receptor 5, but not interleukin-4, attenuate the development of periapical lesions. J Endod 2008;34:31–8.
27. Silva LA, Novaes AB Jr, de Oliveira RR, Nelson-Filho P, Santamaria M Jr, Silva RA. Antimicrobial photodynamic therapy for the treatment of teeth with apical periodontitis: a histopathological evaluation. J Endod 2012;38:360–6.
28. De Rossi A, Rocha LB, Rossi MA. Application of fluorescence microscopy on hematoxylin and eosin-stained sections of healthy and diseased teeth and supporting structures. J Oral Pathol Med 2007;36:377–81.
29. Brown JH, Brenn L. A method for the differential staining of Gram-positive and Gram-negative bacteria in tissue sections. Bull. Johns Hopkins Hosp 1931;48: 69–73.
30. Zhu W, Yang W, He Z, et al. Overexpressing autoimmune regulator regulates the expression of toll-like receptors by interacting with their promoters in RAW264.7 cells. Cell Immunol 2011;270:156–63.
31. Hou L, Sasaki H, Stashenko P. Toll-like receptor 4-deficient mice have reduced bone destruction following mixed anaerobic infection. Infect Immun 2000;68:4681–7.
32. Gelani V, Fernandes AP, Gasparoto TH, et al. The role of toll-like receptor 2 in the recognition of *Aggregatibacter actinomycetemcomitans*. J Periodontol 2009;80: 2010–9.
33. Kawai T, Akira S. TLR signaling. Cell Death Differ 2006;13:816–25.
34. Lang T, Mansell A. The negative regulation of Toll-like receptor and associated pathways. Immunol Cell Biol 2007;85:425–34.
35. Graves DT, Oates T, Garlet GP. Review of osteoimmunology and the host response in endodontic and periodontal lesions. J Oral Microbiol 2011;17:3.
36. Garlet TP, Fukada SY, Saconato IF, et al. CCR2 deficiency results in increased osteolysis in experimental periapical lesions in mice. J Endod 2010;36:244–50.
37. Vernal R, Dezerega A, Dutzan N, et al. RANKL in human periapical granuloma: possible involvement in periapical bone destruction. Oral Dis 2006;12:283–9.
38. Kawashima N, Suzuki N, Yang G, et al. Kinetics of RANKL, RANK and OPG expressions in experimentally induced rat periapical lesions. Oral Surg Oral Med Oral Pathol Oral Radiol Endod 2007;103:707–11.
39. Menezes R, Garlet TP, Letra A, et al. Differential patterns of receptor activator of nuclear factor kappa B ligand/osteoprotegerin expression in human periapical granulomas: possible association with progressive or stable nature of the lesions. J Endod 2008;34:932–8.
40. Moraes M, Lucena HF, Azevedo PR, Queiroz LM, Costa AD. Comparative immunohistochemical expression of RANK, RANKL and OPG in radicular and dentigerous cysts. Arch Oral Biol 2011;56:1256–63.